Biol Fertil Soils (2003) 37:147–153
DOI 10.1007/s00374-003-0581-x

ORIGINAL PAPER

Marc Van Meirvenne · Katrien Maes · Georges Hofman

Three-dimensional variability of soil nitrate-nitrogen in an agricultural field

Received: 18 July 2002 / Accepted: 9 January 2003 / Published online: 22 February 2003

Abstract The aim of this study is to evaluate two different approaches [the layered two-dimensional (2-D) method and a full 3-D approach] to describe the 3-D spatial variability of soil NO_3^--N in the top 1 m of an agricultural field of about 1 ha. NO_3^--N concentrations were determined in layers of 5 cm to a depth of 1 m at 26 locations. These samples were complemented with less intensive sampling at only three depths (0–5, 30–35 and 60–65 cm) at 26 other locations and with topsoil (0–5 cm) samples at another 75 locations. Variogram analysis showed a strong anisotropy when the horizontal dimension was compared to the vertical. A nested model of four structures was used to represent a 3-D variogram. This allowed us to predict the average NO_3^--N concentration for blocks of 5×5 m (horizontally) by 0.05 m (vertically). A cross-validation showed a clear improvement in using the full 3-D interpolation instead of the layered 2-D approach. The full 3-D interpolation seems to be especially useful in situations where knowledge of the 3-D distribution of soil properties is essential to evaluate soil management practices in respect to environmental considerations, like N fertilisation and the subsequent leaching of N to the ground water, or N_2O emissions.

Keywords Geostatistics · Three-dimensional variability · Three-dimensional variogram · Soil nitrate variability

Introduction

Soils are three-dimensional (3-D) bodies with properties that can vary greatly over small distances in every direction. However, soils are generally investigated in only the horizontal dimensions. Even if a 3-D characterisation of the spatial variability of soil properties is the aim, it is often mapped as a set of horizontal layers for a number of soil depths (Oliver and Webster 1987; Samra and Gill 1993). In this approach soil variation is modelled at every depth independently without considering the soil properties above or below it. The major objection to such a layered 2-D approach is that there is a risk that these layers are non-consistent, i.e. discrepancies can occur between layers when put on top of each other. This disadvantage severely limits the usefulness of a layered 2-D approach, especially in situations where the availability of soil nutrients is required in 3-D to model e.g. the plant root-soil interaction (Biondini 2001; Dunbabin et al. 2002). In soil science 3-D studies are quite rare; one exception is Sinowski (1995). However, in mining geology and in studies on environmental contamination, 3-D studies are more common (Journel and Huijbregts 1978; Garcia and Froidevaux 1997; Armstrong 1998).

The aim of this paper is to analyse different approaches used to produce an inventory of soil properties in 3-D. As a case study the soil NO_3^--N content in the top 1 m of an 0.9-ha study area in Belgium was used. NO_3^--N receives a great deal of attention in Belgium due to the environmental restrictions imposed on agriculture to limit nutrient pollution of ground and surface waters. As a result of this, farmers must take care to limit the amount of NO_3^--N residue in the soil profile after harvest. The spatial variability of NO_3^--N has been studied by several authors (Dahiya et al. 1985; Tabor et al. 1985; White et al. 1987, Van Meirvenne and Hofman 1989; Bogaert et al. 2000), but none of them investigated it in 3-D. The 3-D method should give a better insight into variations in N-fertilizer distribution and differences in the mineralization of N from soil organic matter and the possible influence of N fertilizer applications on NO_3^--N leaching and gaseous N losses.

Materials and methods

Theory

The spatial variability of soil properties is mostly studied by using geostatistical methods. These initially characterise the spatial autocorrelation of a variable Z by calculating a measure of the

M. Van Meirvenne (✉) · K. Maes · G. Hofman
Department of Soil Management and Soil Care,
Ghent University, Coupure 653, 9000 Gent, Belgium
e-mail: marc.vanmeirvenne@rug.ac.be

structure of its spatial variance. Therefore, a spatial sampling of Z is conducted which yields n observations $z(x_\alpha)$ with x representing a vector of the spatial co-ordinates (x, y, z) and α=1,...,n. Based on these samples, the semivariance $\gamma(h)$ is calculated (Goovaerts 1997):

$$\gamma(h) = \frac{1}{2n(h)} \sum_{\alpha=1}^{n(h)} \{z(x_\alpha) - z(x_\alpha + h)\}^2 \quad (1)$$

with h being a spatial vector (called lag) separating measurements $z(x_\alpha)$ and $z(x_\alpha+h)$ and $n(h)$ being the number of pairs separated by a given h. A plot of $\gamma(h)$ versus h is called the experimental variogram and a theoretical model is fitted to it in order to characterise the relationship between spatial distance and expected variability in Z. Often a spherical curve is used to model a variogram. It is represented by:

$$\begin{aligned} \gamma_1(h) &= C_1 \cdot \left(\tfrac{3h}{2a} - \tfrac{1}{2}\left(\tfrac{h}{a}\right)^3\right) \quad \text{if } 0 < h \le a \\ \gamma_1(h) &= C_1 \quad \text{if } h > a \end{aligned} \quad (2)$$

with C_1 the sill of the model and a the range. In soil science, a variogram frequently displays discontinuity at the origin, called the "nugget effect", C_0. It is given by:

$$\gamma_0(h) = \begin{cases} 0 & \text{if } h = 0 \\ C_0 & \text{if } h > 0 \end{cases}. \quad (3)$$

In such a situation the variogram model is a combination of these two models: $\gamma(h)=\gamma_0(h)+\gamma_1(h)$. In the situation where the spatial variability is different in different orientations, directional variograms must be calculated yielding an anisotropic variogram model.

To predict the value of Z at any unsampled location x_0 we can use a weighted linear combination of the available samples in a neighbourhood around x_0:

$$z^*(x_0) = \sum_{\alpha=1}^{n(x_0)} \lambda_\alpha z(x_\alpha) \quad \text{with} \quad \sum_{\alpha=1}^{n(x_0)} \lambda_\alpha = 1 \quad (4)$$

where $z^*(x_0)$ is the estimated value of Z at the unsampled location x_0 and λ_α are the $n(x_0)$ weights assigned to the observation points $z(x_\alpha)$ located in the neighbourhood. To ensure that there is no bias in the prediction, the sum of these weights must be 1 (Goovaerts 1997). To obtain these weights the most commonly used algorithm is the ordinary kriging. Sometimes we are more interested in estimating the average value of Z over a given volume (or block) B rather than at a certain point x_0. The predictor thus becomes:

$$z^*(B) = \frac{1}{n(d)} \sum_{\phi=1}^{n(d)} z^*(x_\phi) = \frac{1}{n(d)} \sum_{\phi=1}^{n(d)} \sum_{\alpha=1}^{n(B)} \lambda_\alpha z(x_\alpha) \quad (5)$$

where $n(d)$ is the number of points into which the block was discretised and $n(B)$ is the number of samples in the neighbourhood used to estimate $z^*(B)$. To find these weights the following ordinary block kriging system must be solved:

$$\begin{cases} \sum_{\beta=1}^{n(B)} \lambda_\beta \gamma(x_\alpha - x_\beta) + \psi = \bar{\gamma}(x_\alpha - B) \quad \alpha = 1, ..., n(B) \\ \sum_{\beta=1}^{n(B)} \lambda_\beta = 1 \end{cases} \quad (6)$$

with $\bar{\gamma}(x_\alpha - B)$, the average semivariance between block B and measurement point x_α. Once the weights λ_α have been found, Eq. 5 can be used to predict $z^*(B)$.

3-D kriging implies that the variable was spatially sampled in 3-D to allow the modelling of a 3-D directional variogram. For this we followed the approach presented by Armstrong (1998) who modelled the directional variograms first by considering only pairs located in the horizontal plane or the vertical direction and then combining these directional variograms into one 3-D model. A similar approach was followed by Nash et al. (1988) to combine the horizontal and vertical variograms of soil observations taken along a transect. Whereas the modelling of a 3-D variogram is quite complex (Gringarten and Deutsch 2001), 3-D kriging is straightforward. For kriging we used the GSLIB software (Deutsch and Journel 1998).

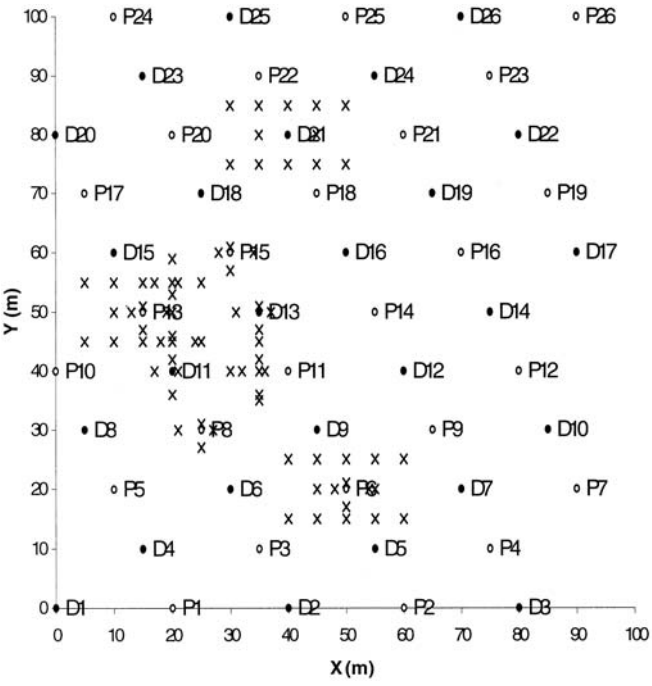

Fig. 1 Sampling locations with sample code (P or D) and number. *Unlabelled crosses* indicate sampling code O

Study area and data set

The study area was a 0.9 ha sub-plot of a larger agricultural field located in the polder area of East Flanders, Belgium. The soils of this area are Fluvents with a weak soil development (A–C profiles). The soil texture is silty clay (42% clay, 43% silt, 15% sand) throughout the profile. In spring 2000 this field was fertilised with NH_4NO3 (27%) at a rate of 90 kg N ha^{-1}, and after the harvest of the crop (winter wheat) in early August, liquid manure was spread at a rate of 40 t ha^{-1} (representing about 180 kg total N ha^{-1}) on 24 August 2000. More details about the study area are provided by Maes (2001).

Soil sampling was conducted on 2–4 October 2000, using three different types of sampling:

1. At 26 locations intensive sampling at 20 depth intervals of 5 cm down to 1 m was conducted using a cylindrical auger (diameter 93 mm) which was drilled into the soil, pulled out and the soil core carefully cut into slices of 5 cm. This yielded 520 soil samples. These samples were coded P.
2. At 26 locations three soil depths (0–5 cm, 30–35 cm and 60–65 cm) were sampled similarly as described under 1. This resulted in 78 soil samples. These samples were coded D.
3. At 75 locations only the top 0–5 cm was sampled, coded O.

Samples P and D were spatially systematically distributed over the study area, but samples D were clustered in order to obtain information about the variability of soil NO_3^--N of samples at a close distance (<10 m) (Fig. 1). In total 674 samples were taken and analysed for NO_3^--N using a NO_3^--specific electrode. A limited number of NH_4^+-N determinations showed background concentra-

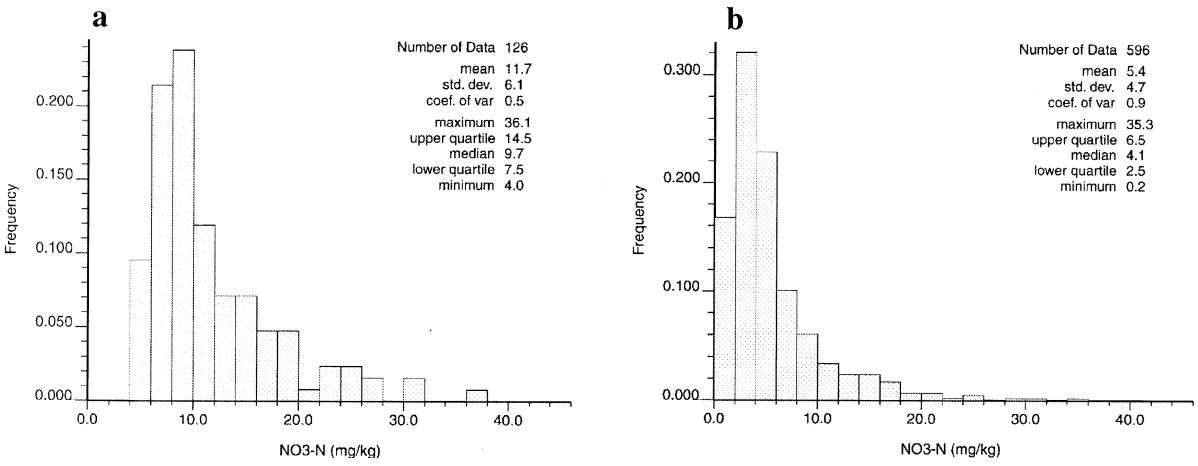

Fig. 2 Histograms of NO_3^--N results determined in all 0- to 5-cm samples (**a**) and in all P and D samples (**b**)

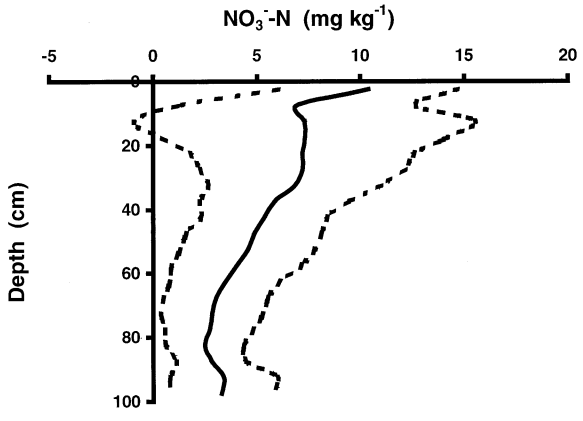

Fig. 3 Average (*unbroken line*) depth profile of NO_3^--N with ±1 SD intervals (*dashed lines*)

tions (<10 kg NH_4^+-N ha^{-1} in the top 30 cm), indicating that most of the NH_4^+-N applied through the liquid manure was already nitrified by the time of sampling.

Results and discussion

Exploratory data analysis

Figure 2 shows the histogram of the NO_3^--N content measured in the 0- to 5-cm samples (Fig. 2a) and the histogram of all P and D samples without the spatially clustered O samples (Fig. 2b). Both histograms indicate a strongly positively skewed distribution, with a median NO_3^--N concentration which was more than twice as large in the 0- to 5-cm layer (median=9.7 mg NO_3^--N kg^{-1}) as in the data set of samples taken at different depth (median=4.1 mg NO_3^--N kg^{-1}) due to the recent fertilisation. Nevertheless, we did not transform the data set to obtain a more symmetrical distribution, to avoid problems related to back-transformation. Some depth samples contained an extremely low NO_3^--N concentration (0.2 mg kg^{-1}) around the detection limit of the NO_3^--specific electrode. These samples contained virtually no NO_3^--N.

Figure 3 shows the average depth profile of NO_3^--N as measured in all samples. It shows the decreasing average N concentration with depth and also the large spread around this average profile. Clearly, the NO_3^--N concentration in this field is highly variable, both in horizontal and vertical directions.

Variogram analysis

Setting up a 3-D variogram of the NO_3^--N distribution proceeded in three steps (Armstrong 1998):

1. Using all 0 to 5 cm samples a horizontal (*X–Y* direction) variogram was modelled.
2. Using all P and D samples a vertical variogram (*Z* direction) was modelled.
3. Combining both previous models into one 3-D model.

Using this approach we assumed that the structure of the horizontal variogram of the 0 to 5 cm samples was representative for all horizontal depth intervals. An insufficient number of samples taken at other depths prevented us from verifying this assumption.

Horizontal variogram

No directional effect of the 0 to 5 cm samples was observed in the horizontal plane. Hence an omnidirectional (i.e. without considering direction) horizontal variogram was calculated and a spherical model with nugget effect (Eqs. 2, 3) was fitted to it with parameters: C_0=3.8 (mg kg^{-1})^2, C_1=14.1 (mg kg^{-1})^2 and a=39.5 m (Fig. 4). A bound structure is observed with a relatively small nugget effect and a spatial range of autocorrelation of almost 40 m.

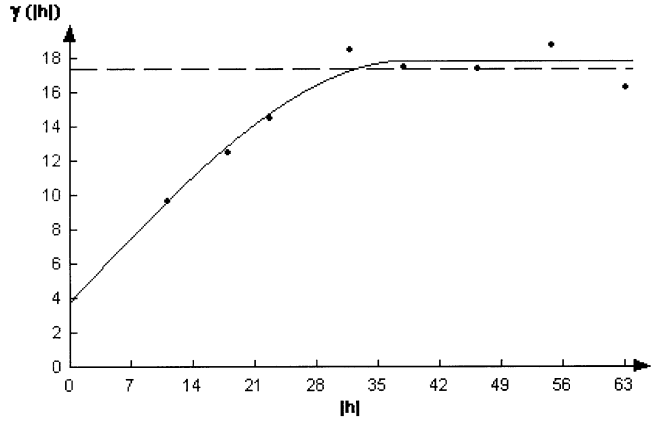

Fig. 4 Omnidirectional horizontal variogram of NO_3^--N calculated from the 0 to 5 cm samples [$\gamma(h)$ is expressed in (mg kg^{-1})^2 and h in m, *dashed line* represents the variance of the data]

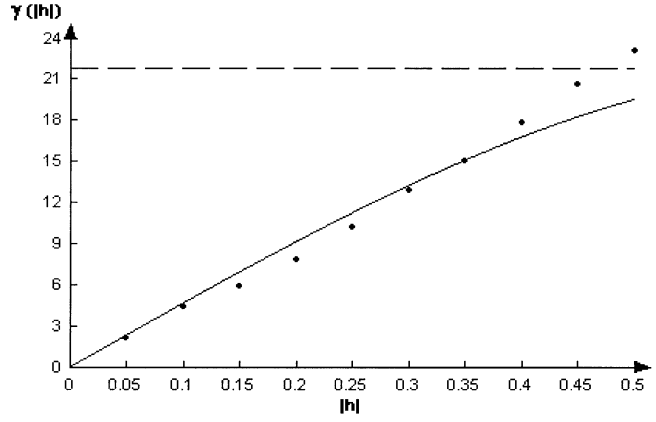

Fig. 5 Variogram of NO_3^--N in the vertical direction; $\gamma(h)$ is expressed in (mg kg^{-1})^2 and h in m; *dashed line* represents the variance of the data

Vertical variogram

Since the maximum depth distance between two observations is 1 m, the vertical variogram could only be calculated over lag distances between 0 and 0.5 m. Figure 5 shows the result and the fitted spherical model with nugget effect. The parameters of this model were: C_0=0.1 (mg kg^{-1})^2, C_1=22.0 (mg kg^{-1})^2 and a=0.7 m, which represents an almost linear increasing function. A range of autocorrelation was not encountered. This indicates that our sampling distance was not large enough to encompass the underlying structure fully. The range parameter of the fitted model (a) should therefore not be interpreted as a measure of the spatial dimension of autocorrelation. In this situation a represents just a model parameter.

3-D combined variogram

By combining the horizontal with the vertical variogram, a 3-D anisotropic variogram was constructed which consisted of an isotropic nugget effect and three spherical models. Table 1 provides the model parameters and Fig. 6 shows a 3-D view of the behaviour of the variogram as a function of a directional angle b with 0º, 180º and 360º being the horizontal direction and 90º and 270º the vertical direction.

The interpretation of the 3-D variogram is as follows:

1. The first nested structure represents a very small 3-D omnidirectional nugget effect (corresponding to the nugget effect of the vertical variogram model).
2. A second nested structure represents a 3-D anisotropic variogram with an omnidirectional sill C_1 of 14.1 (mg kg^{-1})^2 and a directional range. The horizontal range was 39.5 m and the vertical range was 0.7 m (visualised as 70 m in Fig. 6).
3. The third structure adds a nugget effect to the horizontal variogram, but not to the vertical variogram, due to the extremely short range in the horizontal direction (0.000001 m) and the normal range for the vertical variogram (0.7 m). The combination of the first three structures reproduces the horizontal variogram which is omnidirectional in the X–Y plane.
4. The fourth structure increases the sill in the vertical direction without affecting the horizontal direction. This effect is obtained by setting the range in the horizontal direction to a very large value (1,000,000 m), and in the vertical direction to its normal value (0.7 m). The combination of these four structures reproduces the horizontal variogram (Fig. 4) and the vertical variogram (Fig. 5).

This complex nested variogram model allowed us to use a single model to describe the horizontal isotropic behaviour and the strong vertical anisotropy of NO_3^--N in our study area.

Table 1 Parameters of the three-dimensional variogram of NO_3^--N. C_1 Sill, a range

Model	First nested structure Nugget	Second nested structure Spherical	Third nested structure Spherical	Fourth nested structure Spherical
C_0 (mg kg^{-1})^2	0.1	–	–	–
C_1 (mg kg^{-1})^2	–	14.1	3.7	4.2
$a_{horizontal}$ (m)	–	39.5	0.000001	1,000,000
$a_{vertical}$ (m)	–	0.7	0.7	0.7

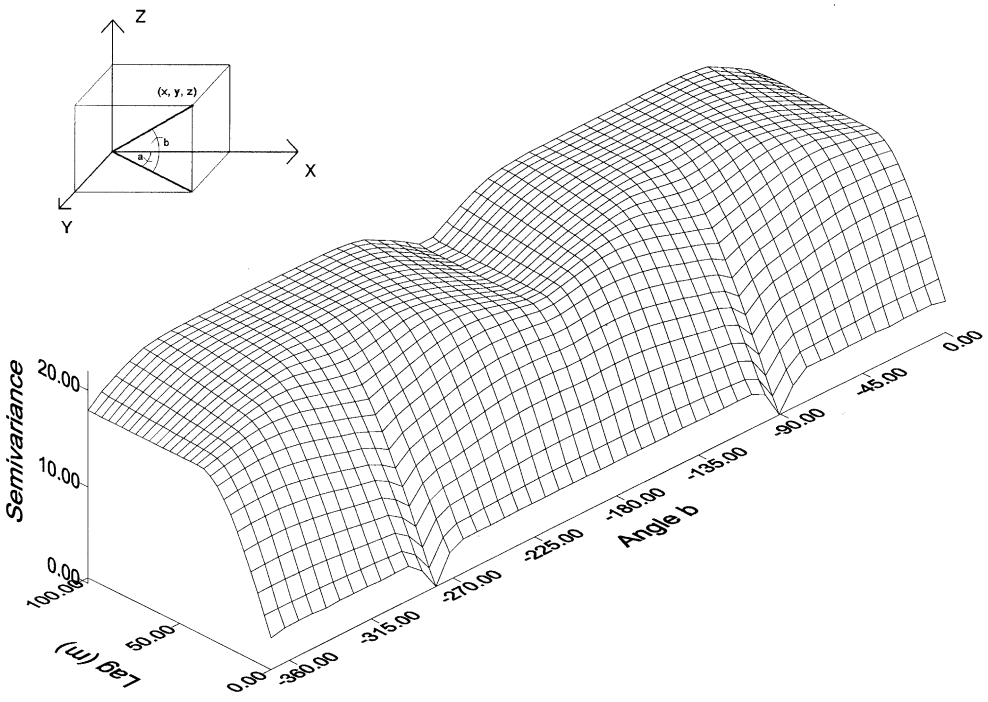

Fig. 6 Visualisation of the three-dimensional (3-D) variogram along angle *b*, representing the angle of a circle oriented perpendicular to the horizontal (*X*–*Y*) plane; the lag distance was exaggerated by a factor of 100 in the vertical (*Z*) direction. For definition of directions and angels see top left-hand figure in which angle *a* represents any horizontal direction (since the horizontal variogram was omnidirectional)

3-D mapping of NO_3^--N

Using ordinary block kriging (Eq. 6), blocks of 5 m (*X*) by 5 m (*Y*) by 0.05 m (*Z*) were interpolated along a 3-D grid of dimension 90 m (*X*) by 100 m (*Y*) by 1 m (*Z*). To avoid the discrepancy in dimension between the horizontal (*X*–*Y*) plane and the vertical (*Z*) direction, *Z* co-ordinates were multiplied by 100 (as in the 3-D variogram model). Each block was subdivided into 4^3 points [$n(d)$ in Eq. 5] and the size of the search neighbourhood was 40 m horizontally and 0.5 m vertically. The minimum number of neighbourhood points [$n(B)$ in Eq. 5] was set to 4 and the maximum to 8.

Figure 7a shows a 3-D view of the results of the 3-D block kriging interpolation (showing typically a smaller range than point observations due to block averaging – compare to Fig. 2). Figure 7b–f illustrates various "sections" through Fig. 7a. These illustrate the large variability (0–15 mg N kg^{-1}) of NO_3^--N within short distances, both horizontally and vertically. Pockets with high N concentrations could be observed both at the surface and at some depths. At other locations the entire soil profile contained only small amounts of NO_3^--N which were homogeneously distributed. This heterogeneous pattern could be explained by a uneven application of the liquid manure or variations in the N-mineralization capacity of the soil.

Comparing the 3-D interpolation with a layered 2-D interpolation

As mentioned before, 3-D variability is often analysed by constructing a set of 2-D layers which are piled on top of each other. This means that for a given layer only observations of that depth are used, whereas in the full 3-D interpolation all measurements taken around the interpolated location are included. The expected gain of using a full 3-D approach is that the studied variable is more consistent between the different depths, but it requires an extra sampling effort in order to construct the 3-D variogram.

To evaluate the importance of this difference between the two approaches, a cross-validation procedure was used, i.e. leaving each observation out in turn and then interpolating at its location using the remaining measurement points. The result is a data set of estimated and measured values at a number of locations. From these results, several indices can be calculated to evaluate the performance of the interpolation method used. The indices we used were:

1. The mean estimation error (MEE):

$$\mathrm{MEE} = \frac{1}{n}\sum_{\alpha=1}^{n}\left(z^*(x_\alpha) - z(x_\alpha)\right)$$

The MEE is a measure of the bias of the estimations. It should be close to zero.

2. The mean square estimation error (MSEE):

$$\mathrm{MSEE} = \frac{1}{n}\sum_{\alpha=1}^{n}\left(z^*(x_\alpha) - z(x_\alpha)\right)^2$$

The MSEE is a measure of the magnitude of the average error. It should be as small as possible.

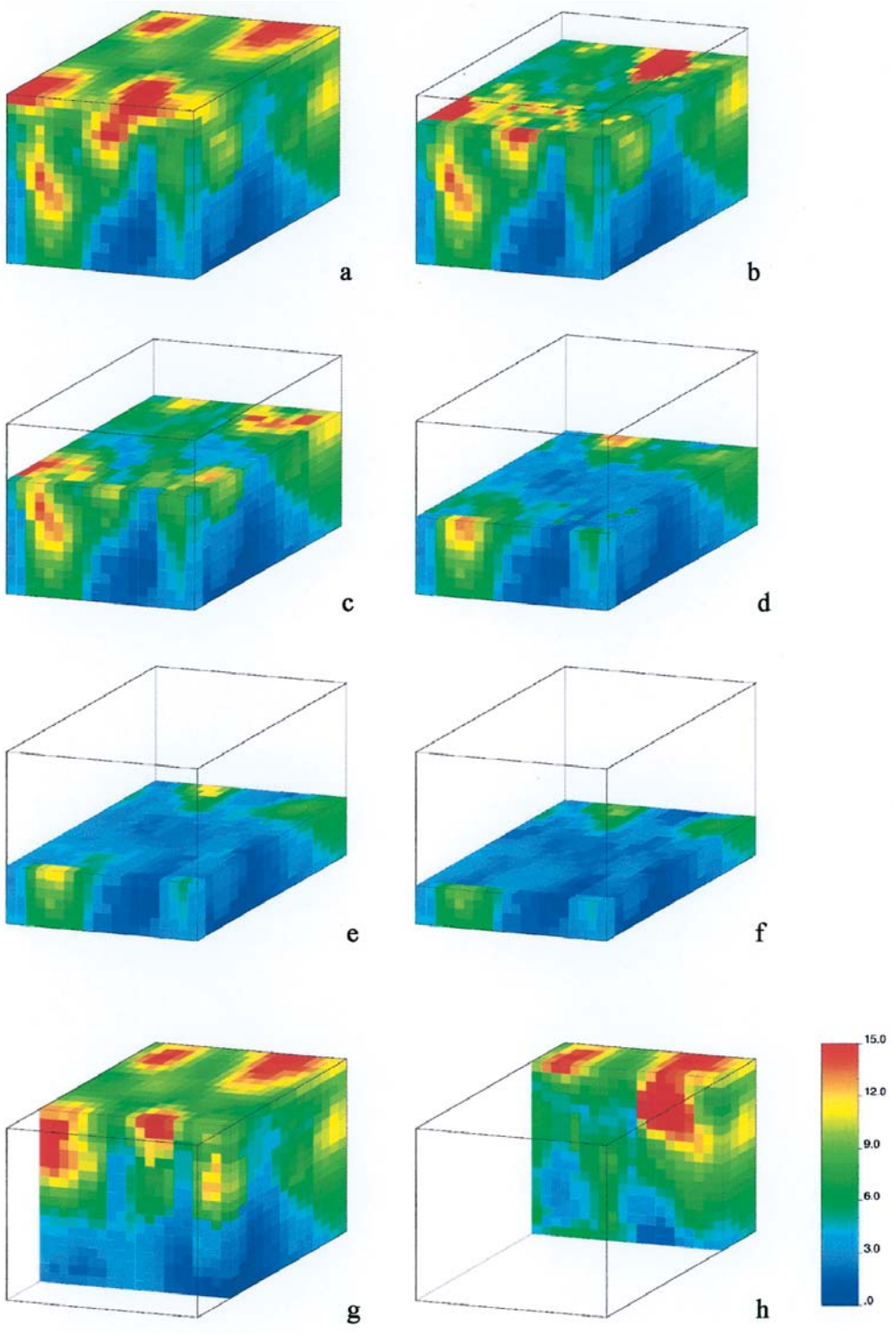

Fig. 7 Interpolated average NO_3^--N (mg kg^{-1})^2 concentration of blocks of 5 m (*X*) by 5 m (*Y*) by 0.05 m (*Z*) for the entire soil volume of 90 m (*X*) by 100 m (*Y*) by 1 m (*Z*) (**a**) and various horizontal (*b–f*) and vertical (*g–h*) sections

3. The Pearson correlation coefficient *r*. It is a measure of the linearity between predicted and measured data. A small MEE and a *r* close to 1 indicate that the predicted values are close to the measured values.

Using only the P and D samples, a horizontal 2-D interpolation was used to conduct a cross-validation of these points, i.e. using only measurements of the same depth as location where an interpolation is required. For this only the horizontal variogram (Fig. 4) was used. This was compared to a full 3-D interpolation where all observations were used to interpolate at each location using the 3-D variogram model (Table 1 and Fig. 6). Figure 8 shows a scatterplot of the estimated versus the measured NO_3^--N concentrations for both approaches.

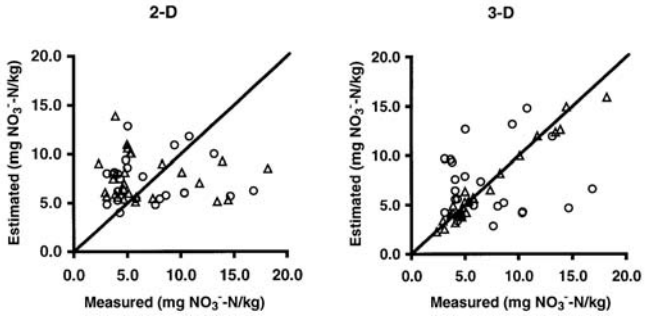

Fig. 8 Results of the cross-validation using a layered 2-D approach (*left*) and a full 3-D approach (*right*) (△ correspond to the P data set, ◯ to the D data set)

The results of the cross-validation indicate that a 3-D interpolation method is a strong improvement on a layered 2-D approach. The MEE remained similar for both approaches (0.20 for the layered 2-D approach and –0.36 mg kg^{-1} for the 3-D approach), but the MSEE was greatly reduced: from 25.67 (mg kg^{-1})^2 for the layered 2-D approach to 16.52 (mg kg^{-1})^2 for the 3-D approach. Also *r* changed from an insignificant, low value for the 2-D approach (–0.09) to 0.49 for the 3-D approach. Especially analysis of the samples of the P data set, i.e. those observed every 5 cm along a profile down to 1 m, benefits from a 3-D approach. This indicates that the improvement was mainly due to the consistent results of the different depth samples taken at the same location. This is important in situations where the investigated variable is subject to vertical migration within the soil profile, like NO_3^--N leaching under a wet climate, or where circumstances are suitable for denitrification.

In conclusion, the data set allowed us to construct a 3-D variogram model which consisted of four nested structures. This variogram model was used to interpolate the average NO_3^--N concentration within blocks of 5 m by 5 m by 0.05 m covering a soil volume of 90 m by 100 m by 1 m. The result illustrated the strong variation in NO_3^--N both in the horizontal and vertical direction. Pockets of high NO_3^--N concentration could be found next to homogeneous profiles with low concentrations at all depths.

A cross-validation indicated that the full 3-D approach was superior to a layered 2-D approach, especially in maintaining consistency between predicted values at different soil depths. This consistency was considered to be important since the NO_3^--N dynamics in wet climates are mainly related to a downward leaching process.

These results suggests that a detailed spatial investigation of NO_3^--N distribution and its evaluation in terms of environmental risk calls for intensive sampling and subsequent 3-D interpolation.

References

Armstrong M (1998) Basic linear geostatistics. Springer, Berlin Heidelberg New York

Biondini M (2001) A three-dimensional spatial model for plant competition in an heterogeneous soil environment. Ecol Model 142:189–225

Bogaert N, Vermoesen A, Salomez J, Hofman G, Van Cleemput O, Van Meirvenne M (2000) The within field variability of mineral nitrogen in grassland. Biol Fertil Soils 32:186–193

Dahiya IS, Anlauf R, Kersebaum KC, Richter J (1985) Spatial variability of some nutrient constituents of an Alfisol from loess: I. geostatistical analysis. J Plant Nutr 148:268–277

Deutsch CV, Journel AG (1998) GSLIB: geostatistical software library and user's guide. Oxford University Press, New York

Dunbabin VM, Diggle AJ, Rengel Z (2002) Simulation of field data by a basic three-dimensional model of interactive root growth. Plant Soil 239:39–54

Garcia M, Froidevaux R (1997) Application of geostatistics to 3D modelling of contaminated sites: a case study. In: Soares A, Gomez-Hernandez J, Froidevaux R (eds) geoENV I – geostatistics for environmental applications. Kluwer, Dordercht

Goovaerts P (1997) Geostatistics for natural resources evaluation. Oxford University Press, Oxford

Gringarten E, Deutsch CV (2001) Variogram interpretation and modeling. Math Geol 33:507–534

Journel AG, Huijbregts CJ (1978) Mining geostatistics. Academic Press, London

Maes K (2001) Modellering van de 3-D variabiliteit van bodemkenmerken. Gevalstudie: nitraat-profiel in een akker. MSc thesis. Ghent University, Ghent

Nash MH, Daugherty LA, Gutjahr A, Wierenga PJ, Nance SA (1988) Horizontal and vertical kriging of soil properties along a transect in southern New Mexico. Soil Sci Soc Am J 52:1086–1090

Oliver M, Webster R (1987) The elucidation of soil pattern in the Wyre Forest of the West Midlands, England. II. Spatial distribution. J Soil Sci 38:293–307

Samra JS, Gill HS (1993) Modeling of variation in a sodium-contaminated soil and associated tree growth. Soil Sci 155:148–153

Sinowski W (1995) Die Dreidimensionale Variabilität von Bodeneigenschaften – Ausmass, Ursachen und Interpolation. Shaker, Aachen

Tabor TA, Warrick AW, Myers DE, Pennington DA (1985) Spatial variability of nitrate in irrigated cotton. II. Soil nitrate and correlated variables. Soil Sci Soc Am J 49:390–394

Van Meirvenne M, Hofman G (1989) Spatial variability of soil nitrate nitrogen after potatoes and its change during the winter. Plant Soil 120:103–110

White RE, Haigh RA, MacDuff JH (1987) Frequency distributions and spatially dependent variability of ammonium and nitrate concentrations in soil under grazed and ungrazed grassland. Fert Res 11:193–208